INSTITUTE FOR FUSION STUDIES

RECEIVED
MAY 13 1996
OSTI

DE-FG03-96ER-54346-742 IFSR #742

Ion Acceleration and Direct Ion Heating in Three-Component Magnetic Reconnection

Y. ONO, M. YAMADA,[a] T. AKAO
Department of Electrical Engineering, University of Tokyo
T. TAJIMA AND R. MATSUMOTO[b]
Institute for Fusion Studies, The University of Texas at Austin,
Austin, Texas 78712 USA

[a] *Present address: Princeton Plasma Physics Laboratory, NJ 08543*
[b] *Present address: Chiba University, Chiba, Japan*

March 1996

THE UNIVERSITY OF TEXAS

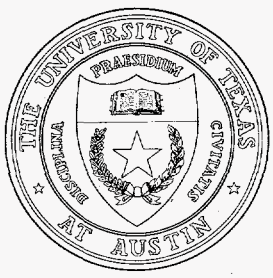

AUSTIN

MASTER
DISTRIBUTION OF THIS DOCUMENT IS UNLIMITED
DK

DISCLAIMER

Portions of this document may be illegible in electronic image products. Images are produced from the best available original document.

Ion acceleration and direct ion heating in three-component magnetic reconnection

Y. Ono, M. Yamada,[a] T. Akao,
Department of Electrical Engineering, University of Tokyo
T. Tajima and R. Matsumoto[b]
Institute for Fusion Studies, The University of Texas at Austin
Austin, Texas 78712 USA

Abstract

Ion acceleration and direct ion heating in magnetic reconnection are experimentally observed during counterhelicity merging of two plasma toroids. Plasma ions are accelerated up to order of the Alfvén speed through contraction of the reconnected field-lines with three-components. The large increase in ion thermal energy (from 10 eV up to 200 eV) is attributed to the direct conversion of the magnetic energy into the unmagnetized ion population. This observation is consistent with the magnetohydrodynamic and macro-particle simulations.

PACS Nos: 52.30.Jb, 96.60.Pb, 52.30.-q, 96.60.-j

[a]Present address: Princeton Plasma Physics Laboratory, NJ 08543
[b]Present address: Chiba University, Chiba, Japan

DISTRIBUTION OF THIS DOCUMENT IS UNLIMITED

Magnetic reconnection has been recognized as an important key physics for topological changes of magnetized plasma configurations. Dynamic reconnection of solar flare is often considered to accelerate plasma particles, leading to the anomalous heating of solar coronas.[1] In the magnetosphere, reconnection at the magnetopause may cause heating of plasma particles and is sometimes related to the aurora phenomena in the polar regions of the earth. In many theoretical models such as Sweet-Parker and Petschek,[2,3] magnetic reconnection is caused by local diffusion of the neutral sheet current flowing along the X-line. It has been generally conceived that diffusion of the neutral current sheet is the main process which transforms the magnetic energy into electron and ion thermal energies, and that it is first transformed to the thermal energy of current carrying electrons through ohmic dissipation of the current sheet and then to the ion thermal energy through electron-ion collisions. However, the outflow jet associated with reconnection has been discussed as an important energy conversion process by several theories, MHD and test-particle simulations.[4,10] Dynamics of field-aligned jet driven by magnetic force of reconnection have been discussed theoretically and computationally, describing its spatial structures and mechanisms.[4,8] Plasma particle motions, such as their $\mathbf{E} \times \mathbf{B}$ drift have also been investigated around the X-point, leading to further understanding of the plasma heating process inside and outside of the field-null region.[9,10] A local X-point structure has been investigated in the laboratory by Stenzel and Gekelman, using a thin electrode discharge-current channel.[11] The electrostatic probe measurement was used to verify the 2-D plasma flow of reconnection. However, heating and acceleration characteristics of reconnection such as its anomalous energy conversion to ions are left unsolved.

An important question has been also raised whether direct ion heating is possible during magnetic reconnection. Ion temperature T_i is often observed to be higher than electron temperature T_e, in some fusion plasmas, such as Reversed Field Pinches (RFPs)[12] and

spheromaks.[13] Mechanisms for the anomalous ion heating have been widely investigated, in terms of their magnetic fluctuations. However, their multiple reconnection points and limited diagnostics have prevented further elucidation of its cause and mechanism.

This paper describes the first clear evidence of direct ion heating of single magnetic reconnection, based on a laboratory experiment on toroidal plasma merging. Its interpretation is aided by computer simulations. The plasma merging experiment and corresponding numerical simulations have verified important steps of the direct ion heating: (1) ion acceleration during magnetic reconnection, (2) its resultant energy-transfer process to the ion thermal energy.

In the present experiment, ion acceleration in the toroidal direction and a large increase in the ion temperature are measured around a single reconnection point. Two merging spheromaks with equal but oppositely directed toroidal magnetic field B_t are used to produce an axisymmetric X-point line. The merging angle of reconnecting field-lines is always about 180°.[14,15] The TS-3 merging device[15] is used to produce two spheromaks along the center axis, and to merge them together in the axial direction. Its cylindrical vacuum vessel with the diameter of 0.8 m and the length of 0.9 m has two internal poloidal field (PF) coils and two sets of eight pair electrode rings to produce poloidal and toroidal magnetic fluxes of the two initial spheromaks, respectively. A 2-D array of magnetic probes is located on the r-z-plane of the vessel to measure 2-D contours of poloidal and toroidal magnetic fields on a single discharge. These data are used to calculate poloidal flux (Ψ) contours and magnetic energy evolutions of the merging toroids. Doppler width of H_β line and Doppler shifts of C_{II} line (and H_β line for confirmation) are used to measure radial profiles of ion temperature and velocity on the midplane. Figures 1(a) and (b) show the axial profiles of B_t at $r = 18$cm and the poloidal flux contours during the reconnection of the two merging spheromaks. The two spheromaks with opposite B_t have plasma currents of ~ 30 kA and major and minor radii of 18cm and 12cm, right after their formations (at $t = 10\mu$sec). At

$t = 17.5\mu$sec, two magnetic axes merge completely, indicating that the reconnection time is less than 10μsec. Note that the B_t profile offers an overshoot or an oscillation after the completion of the reconnection. Until $t = 17.5\mu$sec, the polarity of B_t is still kept as they are initially given by the two spheromaks: positive on the left-hand side and negative on the right-hand side. Figure 1(c) shows the radial profiles of the global ion velocity in the toroidal direction measured on the midplane. From $t = 12.5\mu$sec to 22.5μsec, the global ion velocity is observed to increase in both edge regions. The largest velocity shear is observed at $t = 22.5\mu$sec, that is $\sim 3\mu$sec after the B_t profile passes the zero-line and changes its polarity: negative on the left-hand side and positive on the right-hand side. The ion velocity is positive for $r > 18$cm and negative for $r < 18$cm, in agreement with the polarity of the field-line motion observed in Fig. 1(a). Both measurements indicate that the inner-halves and outer-halves of the reconnected field-lines accelerate plasma ions oppositely in the toroidal direction. The maximum global ion velocity ~ 12km/sec observed at $r = 22$cm is about 1 to $\frac{1}{3}$ of the field-line velocity $\sim 15 - 45$km/sec that is order of the local Alfvén speed calculated from $n_i \sim 2 \times 10^{20}\,\mathrm{m}^{-3}$ and $B = 0.1 - 0.3$kG. Local ion velocity around the X-point is probably larger than the measured global velocity, because not the local upstream flow but the global downstream flow mostly oriented to the toroidal direction is measured with the resolution of 3cm in the r and z-directions that is comparable or larger than the width of compressed current sheet. The velocity shear is observed to gradually vanish after $t = 22.5\mu$sec. The B_t field with reversed polarity also starts decreasing after $t = 25\mu$sec, suggesting that the oppositely directed field-line motion decreases the ion velocity. This overshoot or oscillation of the reconnected field-lines is observed mostly once or rarely twice. Finally, the B_t profile relaxes uniformly to zero at $t = 40\mu$sec, indicating the formation of a field-reversed configuration (FRC).[16]

The acceleration of plasma ions is connected with a large increase in ion temperature T_i. Figure 2 shows the radial profiles of ion temperature T_i measured on the midplane. In the

initial reconnection phase (at $t = 11\mu$sec), T_i is uniformly small ~ 10 eV. Right after the magnetic reconnection is completed, T_i starts increasing rapidly at $t = 15\mu$sec and reaches the peak value as large as 200 eV at $t = 23\mu$sec. Around this time, the velocity shear also reaches the maximum amplitude during the first overshoot of the reconnected field-lines. As shown in Fig. 2, the magnetic reconnection increases significantly the ion thermal and kinetic energies, producing the macroscopic reconnection outflow observed in Fig. 1. By the help of large ion viscosity in the field-annihilated region, the overshoot motion of field-lines, especially that opposite to the ion flow, possibly contributes to thermalization process of the ion kinetic energy. The energy flow of our reconnection experiment is illustrated in Fig. 3. Based on the T_i measurement as a function of poloidal flux Ψ, the total increase in the ion thermal energy $W_{i,th}$ is estimated to be ~ 180 J (± 30 J). This value is as large as 80% ($\pm$ 20%) of the dissipated magnetic energy $W_m \sim 230$ J (± 20 J) (whole toroidal magnetic energy and part of poloidal magnetic energy) during the reconnection. This fact indicates that the dissipated magnetic energy is transformed mostly into the ion thermal energy. However, the magnetic energy dissipation $W_{\rm sheet}$ of the neutral current sheet is estimated to be as small as 20 J. This value is calculated from the measured 2-D magnetic field contours, using $W_{\rm sheet} \sim 2\pi R\delta LEj\tau_{\rm rec}$, where R is the radius of the toroidal X-point line, δ and L are the width and the length of the current sheet, E and j are the toroidal electric field and the toroidal current density at the X-point, and $\tau_{\rm rec}$ is the reconnection time.[15] These comparisons lead us to conclude that the significant ion heating is made directly by the slingshot motion in the bulk plasma and not by the dissipation of the neutral sheet current. The direct energy conversion is probably explained by the ion viscosity heating in the process of forming velocity shear and not by the finally formed global ion flow itself whose energy is less than 20 J. They can be compared with the following two numerical simulations, which will be described only to the extent to elucidate the above physical phenomenon in this experimental paper.

A three-dimensional (3D) MHD simulation of two merging flux tubes with counterhelicity magnetic fields has been carried out by using 3D resistive MHD code based on the modified Lax-Wendroff method[17] with artificial viscosity.[18] The Ohm's law $\mathbf{E} = -\mathbf{v}\times\mathbf{B}+\eta\mathbf{J}$ is adopted where the resistivity η is parametrized by the magnetic Reynolds number R_m. The number of grid points used for simulation is $(N_r, N_\theta, N_z) = (42, 42, 82)$. Toroidal and poloidal magnetic fields of the flux tubes are $B_t = B_0 J_0(2r/a)$ and $B_p = B_0 J_1(2r/a)$, respectively, where J_0 and J_1 are Bessel functions. We assume spatially uniform resistivity with $R_m = 10^3$. As is the case of experiment,[14,15] distinct from the cohelicity case, two tubes with counterhelicity merge rapidly on the order of tens of the Alfvén times ($\tau_A = a/v_A$). Figure 4 shows the isosurfaces of magnetic field strength (white), isosurfaces of $v_t = \pm 0.3 v_A$ (blue and orange), velocity vectors (green), magnetic field lines (red) at (a) $t = 86\tau_A$, and (b) $t = 100\tau_A$. Once the merging starts and Y-points appear, the rapid reconnection progresses and the separation of two Y-points quickly enlarges. During this stage, the originally nearly 180° oppositely directed field lines in the $\theta - R$ plane rapidly reconnect and as they do, these field lines now direct in the z-direction (see the magnetic field lines in Fig. 4(a)). Upon this explosive process, the fluid offers a slingshot motion in the toroidal direction, as seen in the velocity vectors in Fig. 4. The maximum velocity of the fluid is $\sim 0.8\, v_A$. The velocity isosurface in Fig. 4(a) also shows that the direction of the slingshot velocity changes with R, consistent with the experiment. The magnetic reconnection occurs in the tilted plane with nearly no magnetic field normal to this plane, in contrast to the cohelicity case, as shown in the schematic pictures in Fig. 1. Once reconnection occurs on this particular plane, the contraction of the reconnected field-lines accelerates the plasma section with the ellipsoidal cross-section in the toroidal direction (with a tilt toward the R-direction). By this time, the next action of reconnection of two field lines in the opposite toroidal directions occurs in the inner part of the two Y-points that are now rapidly receding away. Again the above process repeats for the next slice of the plasma. The receding ellipsoidal plasma slice oscillates due

to its magnetic tension (primarily Alfvén oscillations), thus causing oscillating B_t and v_t as a result. These seem to well correlate with what we observe in Fig. 1. Note that the plasma thermal energy increases significantly right after the reconnection. The increment of thermal energy is much larger than the kinetic energy, revealing the direct plasma heating observed in Fig. 2.

In the counterhelicity case, there appears a substantial region of null or very weak field, where ions are unmagnetized. It is here that the full description of heating needs kinetic dynamics and also here that significant direct ion momentum transfer and subsequent heating take place. Thus the slingshot oscillations and acceleration/heating are investigated by a kinetic macro-particle simulation. Although the parameters of kinetic simulation cannot quantitatively match those of experiment and MHD simulation, a similar behavior is reproduced. As noted above, the dynamics in the appropriate $\theta - z$-plane is essentially 2-$\frac{1}{2}$-dimensional (i.e. the morphology depends on two-dimensions in this plane, while the vectors $\mathbf{v}$ can be pointed not only in the plane but also normal to this). This electromagnetic macro-particle simulation scheme described in Ref.[19] includes both ion and electron dynamics, allowing for finite Larmor radius effects and charge separation effects. Realized reconnection is basically collisionless (its magnetic Reynolds number $S > 10^4$), but may not be so highly collisionless as that in the magnetosphere, because some screened coulomb collisions remain. What we performed is such 2-$\frac{1}{2}$-dimensional coalescing flux tubes where two tubes straight in the θ-direction merge together in the z-direction without magnetic field normal to the plane, thus causing 180° reconnection.[8] This setup is the same as Ref.[8]. Under this condition, magnetic fields exhibit slingshot oscillations (not shown here) after reconnection. Figure 5 shows the time history of ion energy in the coalescing direction (z) and electron energy in the θ direction. (Since electrons are magnetized, their energy in the z-direction does not exhibit strong bulk heating, as seen in ions.) Where no magnetic field exists in the counterhelicity case, coalescing flows of ions interpenetrate each other and

rapidly mix. This is one major process of ion momentum transfer through ion viscosity. Electrons can not freely mix and thus no bulk heating of electrons results as they are still magnetized and move through the $\mathbf{E} \times \mathbf{B}$ motion. Since the region, which is encircled by the new poloidal fields and does not contain much field inside, is substantial (not a just X-point or X-line), so that this interpenetrating ion momentum transfer takes place over a substantial finite volume. This is the most probable reason why the dissipated toroidal magnetic energy is transformed mostly to ions and not to electrons, in agreement with the experiment mentioned.

In summary, a series of experiments and simulations elucidates the ion acceleration and direct ion heating effects in the three-component reconnection. Two important aspects of the direct ion acceleration and heating are consistently observed: contraction of reconnected field-lines accelerates plasma ions toroidally up to order of the Alfvén velocity, producing a large velocity shear, and at the same time, this acceleration process heats plasma ions directly and selectively, converting the dissipated magnetic energy mostly into the ion thermal energy. It is noted that the large local ion velocity shear appears in the presence of large viscosity force. The work made against this viscosity force is transformed into the ion thermal energy. This ion momentum transfer is large because ions are unmagnetized in a wide region where the counterhelicity reconnection annihilates the toroidal field. This heating mechanism is very small for magnetized electrons, leading to a possible explanation for the $T_i \gg T_e$ characteristics, observed in our result. This bulk heating mechanism may give an additional factor in explaining the study of the coronal heating whose power is much larger than sheet current dissipation. The observed selective ion heating is also consistent with the RFP experiments whose reconnection has field-line-merging angles as large as 180°.

Acknowledgments

We would like to thank Dr. R. Kulsrud for useful discussions and Dr. M. Katsurai and the TS-3 group for experimental supports and discussions.

This work was supported in part by the U.S. Dept. of Energy contract No. DE-FG03-96ER-54346.

DISCLAIMER

This report was prepared as an account of work sponsored by an agency of the United States Government. Neither the United States Government nor any agency thereof, nor any of their employees, makes any warranty, express or implied, or assumes any legal liability or responsibility *for the accuracy, completeness, or usefulness of any information, apparatus, product,* or process disclosed, or represents that its use would not infringe privately owned rights. Reference herein to any specific commercial product, process, or service by trade name, trademark, manufacturer, or otherwise does not necessarily constitute or imply its endorsement, recommendation, or favoring by the United States Government or any agency thereof. The views and opinions of authors expressed herein do not necessarily state or reflect those of the United States Government or any agency thereof.

REFERENCES

[1]S. Tsuneta *et al.*, Publ. Astron. Soc. Japan **44**, L63 (1992); K. Shibata *et al.*, *ibid* **44**, L173 (1992).

[2]E.N. Parker, J. Geophys. Res. **62**, 509 (1957).

[3]H.E. Petschek, in *AAS-NASA Sym. Phys. Solar Flares*, (U.S. Gov. Printing Office, Washington D.C., 1964), p. 425.

[4]D. Biskamp, Phys. Fluids **29**, 1520 (1986).

[5]E.R. Priest and L.C. Lee, J. Plasma. Phys. **44**, 337 (1991).

[6]L.C. Lee and Z.F. Fu, J. Geophys. Res. **91**, 6807 (1992).

[7]K. Shindler and J. Birn, J. Geophys. Res. **92**, 95 (1987).

[8]T. Tajima and J.-I. Sakai, Sov. J. Plasma Phys. **15**, 519 (1989); J.-N. Leboeuf *et al.*, Phys. Fluids **25**, 784 (1982).

[9]G.R. Burkhart *et al.*, J. Geophys. Res. **95**, 18833 (1990).

[10]R.W. Moses *et al.*, J. Geophys. Res **98**, 4013 (1993).

[11]R. Stenzel *et al.*, J. Geophys. Res. **87**, 111 (1982); W. Gekelman and H. Pfister, Phys. Fluids **31**, 2017 (1988).

[12]K.F. Schenberg *et al.*, in *Plasma Phys. Cont. Nucl. Fus. Res. 1988* (IAEA, Vienna, 1989), Vol. 2, p. 419; E. Scime *et al.*, Phys. Fluids **4**, 4062 (1992).

[13]J. C. Fernandez *et al.*, Nucl. Fusion **30**, 67, (1990); M. Yamada *et al.*, Phys. Fluids B **2**, 3074 (1990).

[14]M. Yamada *et al.*, Phys. Rev. Lett. **65**, 721 (1990).

[15]Y. Ono *et al.*, Phys. Fluids B **5**, 3691 (1993).

[16]Y. Ono *et al.*, in *Plasma Phys. Cont. Nucl. Fusion Res. 1992* (IAEA, Vienna, 1993), Vol. 2, p. 619; Y. Ono, Trans. Fusion Tech. **27**, 369 (1995).

[17]E. Rubin and S.Z. Burstein, J. Comput. Phys. **2**, 17 (1967).

[18]R.O. Richtmyer and K.W. Morton, *Differential Methods for Initial Value Problems (2nd ed.)*, (Interscience, New York, 1967), Chap. 13.

[19]C.K. Birsall *et al.*, in *Methods in Computational Physics*, edited by B. Alder *et al.*, (Academic Press, New York, 1970), Vol. 9, p. 241.

FIGURE CAPTIONS

Fig. 1. Axial profiles of toroidal magnetic field B_t at $r = 18$cm (a), poloidal flux contours on the r-z-plane (b), and radial profiles of ion global velocity V in the toroidal direction on the midplane (c) during the reconnection of two merging spheromaks with equal but oppositely directed B_t. A B_t probe array is located axially at $r = 18$cm that passes approximately the position of the X-point.

Fig. 2. Radial profiles of ion temperature T_i measured on the midplane.

Fig. 3. Energy flow pattern of magnetic reconnection with $\theta \sim 180°$. The magnetic energy is transformed mostly into the ion thermal energy not by the neutral current sheet dissipation but by the direct energy conversion process.

Fig. 4. The result of 3-D MHD simulation of the reconnection between counterhelicity flux tubes. The white surfaces show the isosurface of magnetic field strength. The blue and orange surfaces show the isosurfaces of positive and negative toroidal velocities ($v_t = \pm 0.3 v_A$), respectively. The green arrows show velocity vectors. The red curves are magnetic field lines. (a) $t = 86\tau_A$, (b) $t = 100\tau_A$.

Fig. 5. The result of 2-1/2 dimensional EM (electromagnetic) kinetic macro-particle simulation of counterhelicity coalescence: ion temperature in the z (coalescing) direction and electron temperature in the θ direction.

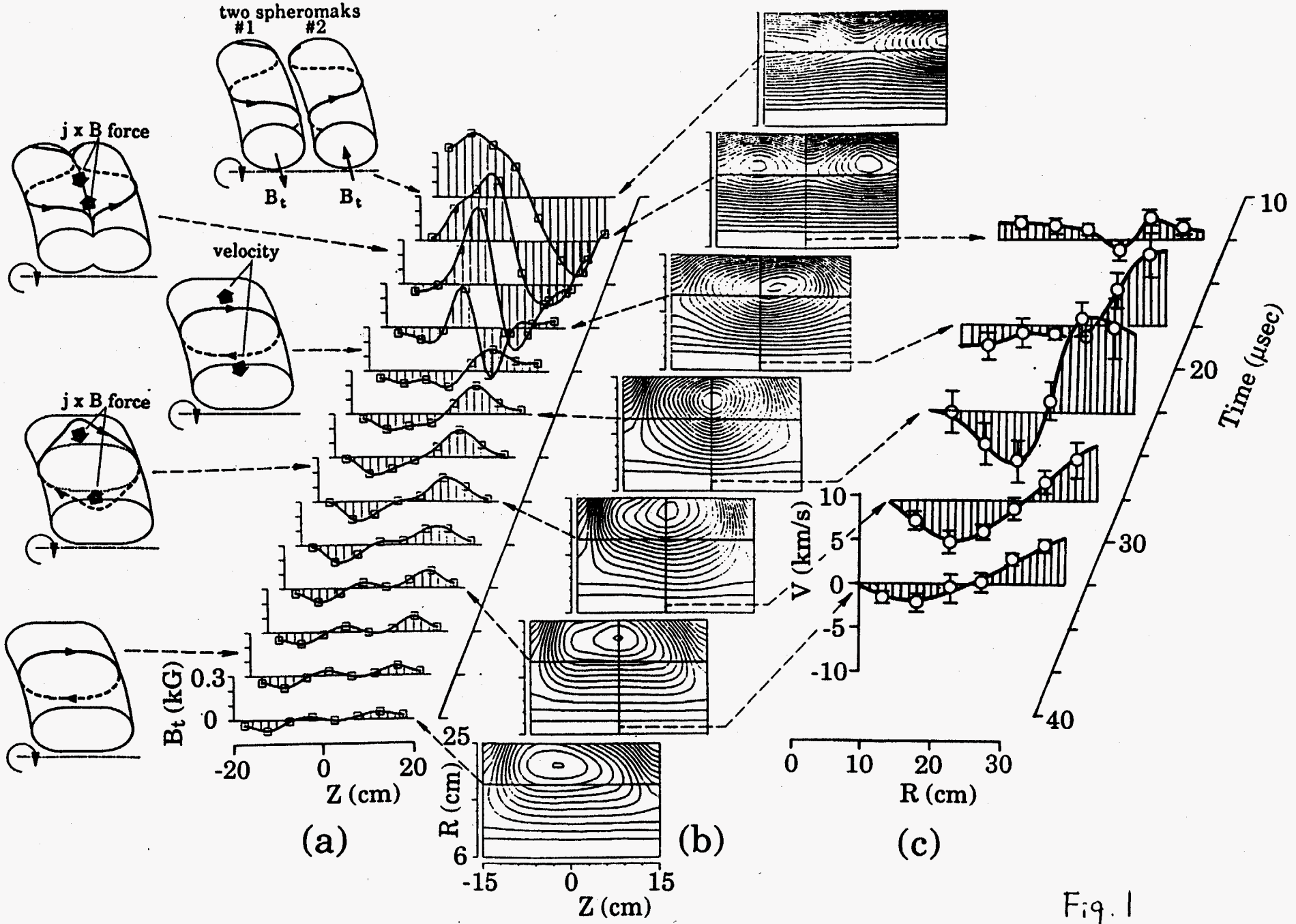
two spheromaks
#1
#2
B_t
B_t
j x B force
velocity
j x B force
B_t (kG)
0.3
0
-20
0
20
Z (cm)
(a)
R (cm)
25
6
-15
0
15
Z (cm)
(b)
V (km/s)
10
5
0
-5
-10
0
10
20
30
R (cm)
(c)
10
20
30
40
Time (μsec)

Fig. 1

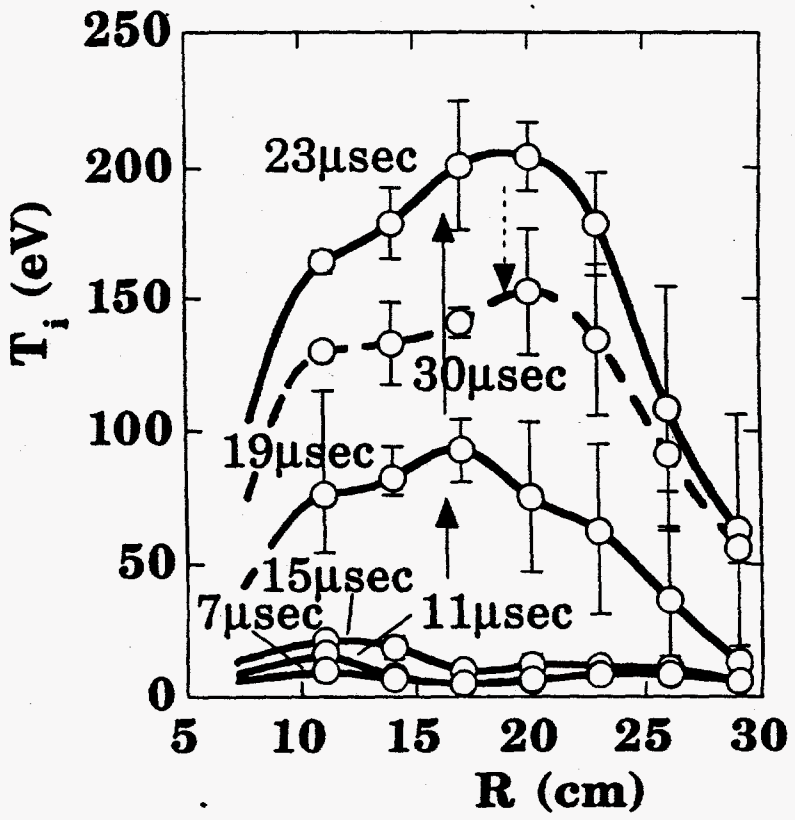
250
200
150
100
50
0
T_i (eV)
23μsec
30μsec
19μsec
15μsec
7μsec
11μsec
5
10
15
20
25
30
R (cm)

Fig. 2

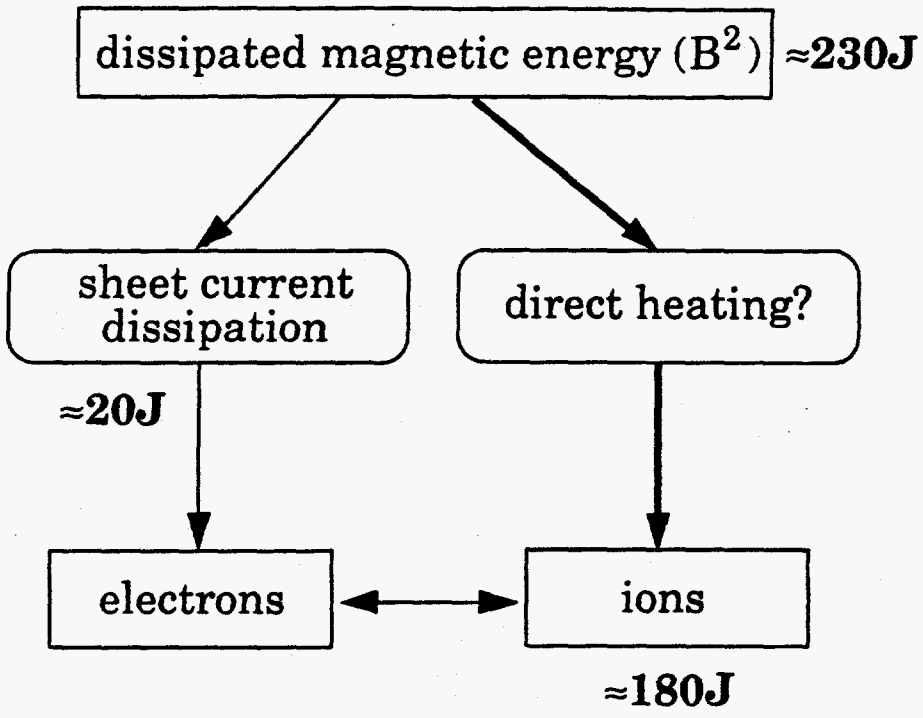
dissipated magnetic energy (B^2)
≈230J
sheet current dissipation
direct heating?
≈20J
electrons
ions
≈180J

Fig. 3

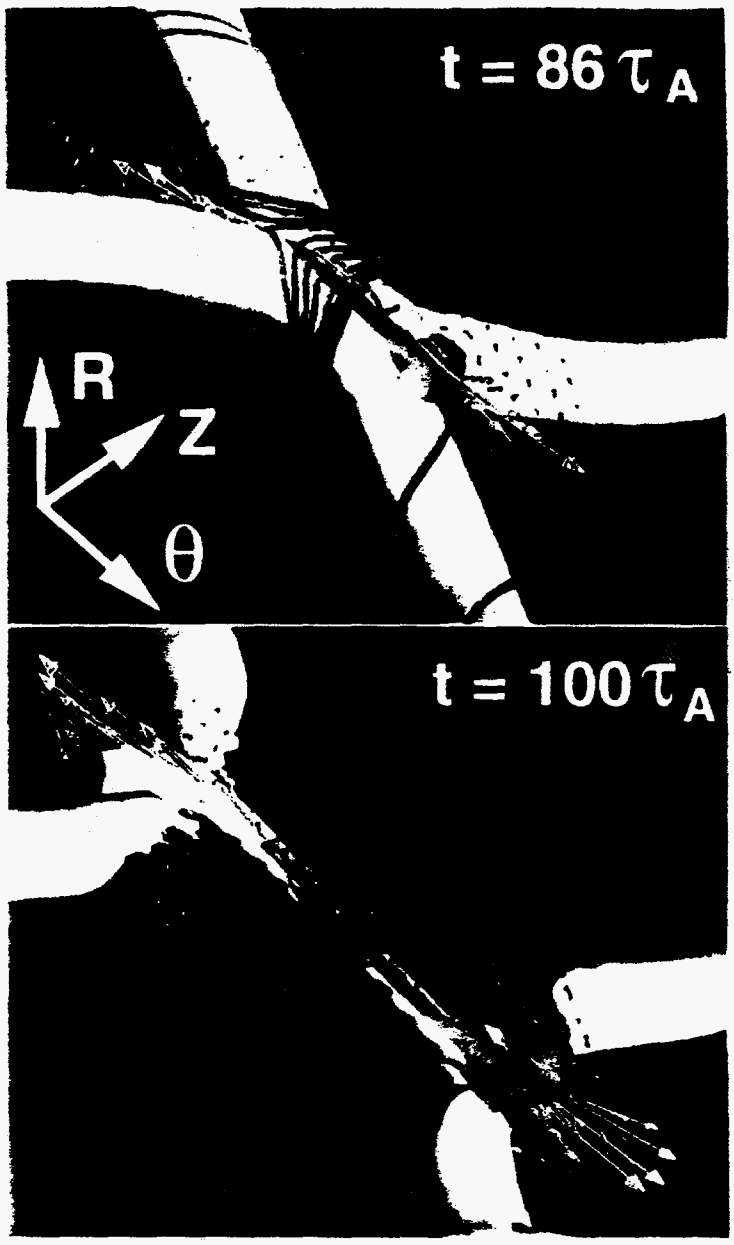

Fig. 4

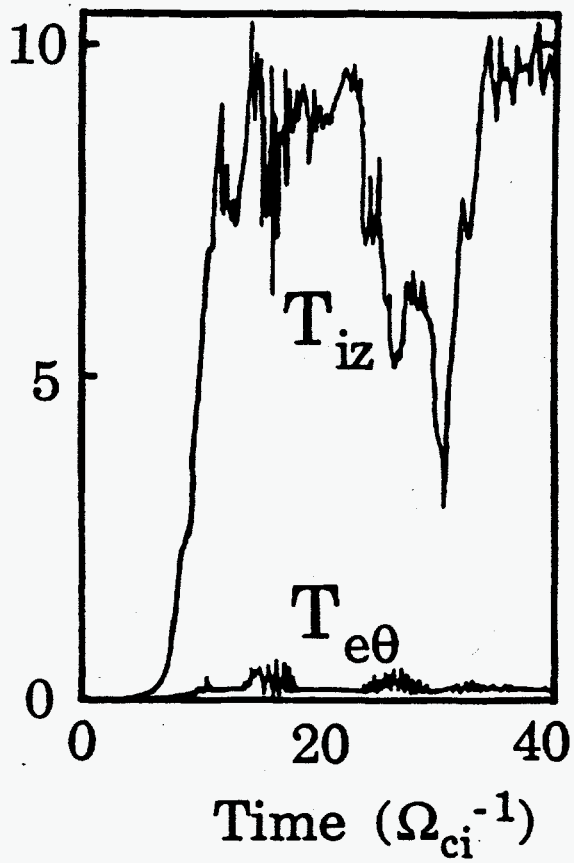

Fig. 5